

# Talin binds to actin and promotes filament nucleation

S. Kaufmann, T. Piekenbrock, W.H. Goldmann, M. Bärmann and G. Isenberg

*Biophysics Department E22, Technical University of Munich, D-8046 Garching, Germany*

Received 2 April 1991

Platelet talin binds to actin *in vitro* and hence is an actin binding protein. By four different non-interfering assay conditions (fluorescence, fluorescence recovery after photobleaching, (FRAP), dynamic light scattering and DNase-I inhibition) we show that talin promotes filament nucleation, raises the filament number concentration and increases the net rate of actin polymerization but has no inhibitory effect on filament elongation. Binding of talin to actin occurs at a maximal molar ratio of 1:3 as determined by fluorescence titration under G-buffer conditions. The overall binding constant was  $\approx 0.25 \mu\text{M}$ .

Talin; Platelet; Actin polymerization

## 1. INTRODUCTION

Talin is a protein that is believed to mediate cytoskeleton-membrane interactions [1,2]. In platelets, the redistribution of talin from the cytoplasm towards the plasma membrane during activation [3,4] reflects an involvement of this protein in rapidly induced cellular shape changes [5]. Insertion of talin into membranes is provided by a selective interaction with lipid bilayers [6]. The binding to actin on the other hand would be of importance for linking the actin network to the plasma membrane. So far, evidence for a direct interaction between talin and actin was lacking although it has been observed that talin influences actin polymerization in some way [7]. Here, we report that talin binds to actin *in vitro* and affects actin polymerization by a non-capping but strongly nucleation promoting activity.

## 2. MATERIALS AND METHODS

### 2.1. Proteins

Platelet talin was purified as described [6]. For the last purification step, a gel filtration column, the ionic strength was raised to 500 mM KCl to avoid precipitation during concentration. Actin was extracted from skeletal muscle acetone powder [8] and further purified by gel filtration [9]. Protein concentrations were determined according to Bradford [10] and the purity was analyzed on SDS mini slab gels [11]. NBD (7-chloro-4-nitro-benzo-2-oxa-1,3-diazole)-actin was prepared following the protocol of Detmers et al. [12].

### 2.2. Fluorescence spectroscopy

The fluorescence increase of polymerizing actin was measured in a SPEX Fluorolog 1680 0.22 double spectrometer at the excitation and emission wavelength of 480 and 530 nm, respectively. The actin concentration (1.5  $\mu\text{M}$ ; 95% actin plus 5% NBD-actin) was kept constant

in a total volume of 0.5 ml. Polymerization was started by adding F-actin buffer: 2 mM Tris-HCl pH 8.0; 0.2 mM  $\text{MgCl}_2$ ; 100 mM KCl; 0.2 mM  $\text{CaCl}_2$ ; 0.2 mM ATP; 0.2 mM DTT; 0.005%  $\text{NaN}_3$ .

### 2.3. Fluorescence recovery after photobleaching (FRAP)

The 1 W power output 488 nm spectral line of an argon ion laser was used to bleach a spot with a diameter of 10  $\mu\text{m}$  [13]. Fluorescence recovery in the bleached area was recorded by a photomultiplier using a 1000 times weaker observation beam than fluorescence excitation. FRAP experiments were performed in F-actin solutions (0.1 mg/ml containing a 20% weight fraction of NBD-actin) which were allowed to polymerize for 2 h at 25°C in the presence of talin at various concentrations. Fluorescence recovery was recorded in intervals of 5–10 min per measurement, yielding a recovery of 50–90%. Each measurement was repeated five times and an average was recorded. Data fits were carried out according to the following algorithm:

$$f(t) = \exp(-2 \tau_d/t) [I_0(2 \tau_d/t) + I_1(2 \tau_d/t)]$$

$$F(t) = F(0) + F_\infty - F(\infty)f(t)$$

Where  $\tau_d$  is the relaxation time  $\tau_d = r^2/4D$ ,  $r$  being the radius of the bleached spot and  $D$  the diffusion coefficient.  $I_0$  and  $I_1$  are modified Bessel functions of zero and first order.  $F(t)$  is the measured fluorescence yield at time  $t$  after bleaching and  $F_\infty$  the fluorescence before bleaching. In a first data fit,  $\tau_d$  and  $F(\infty)$  were adjustable, in a second fit  $F(\infty)$  was preset in a way that the mobile fraction equalled:

$$[F(\infty) - F(0)]/[F_\infty - F(0)] = 0.9.$$

### 2.4. Dynamic light scattering

The experimental setup has been described in detail by Schmidt et al. [14]. The following modifications were made: the 514.5 nm spectral line of an Innova 70-4 (coherent laser) served as light source, and correlation functions were recorded by an ALV3000 (ALV, Langen) correlator on a blockwise logarithmic time scale. Cylindrical test tubes of 1.5 cm diameter were cleaned exhaustively with deionized filtered water. In dust-free environment, water, F-buffer, talin at various concentrations and actin (0.1 mg/ml) were filtered into the tubes through pre-cleaned Millex-GV filters (Millipore). All samples were stored overnight at 4°C in order to achieve a fixed state. Light scattering experiments were performed at 10°C in a time sequence of 4 min duration. The scattering intensity remained constant within the measuring time.

Correspondence address: G. Isenberg, Biophysics Dept. E22, Technical University of Munich, D-8046 Garching, Germany

### 2.5. DNase-I inhibition assay

The amount of free G-actin under polymerization conditions in the presence and absence of talin was determined by the DNase-inhibition assay [15]. Calf thymus DNA (80  $\mu\text{g}/\text{ml}$ ) was dissolved in 0.1 M Tris-HCl, pH 7.5, 4 mM MgSO<sub>4</sub> and 1.8 mM CaCl<sub>2</sub> by gentle stirring at 4°C for 24–48 h. The insoluble DNA was removed by centrifugation at 30000  $\times g$  and the supernatant was stored at -20°C. DNase I solution (0.1 mg/ml in 50 mM Tris-HCl pH 7.5, 0.2 mM CaCl<sub>2</sub> and 0.01 mM PMSF) was prepared prior to use. For determination of DNase I inhibition, G-actin and talin, dialyzed into G-buffer were preincubated in a molar ratio of 1:1 at 25°C in F-buffer. Each sample was thoroughly mixed with DNase I in a constant molar ratio. Aliquots of these mixtures containing 24.8 nM DNase I solution were transferred into a cuvette and mixed with 1 ml prewarmed (25°C) DNA solution for measuring the hyperchromicity at 260 nm for 30 s. Increase in absorbance was measured with an Perkin-Elmer Lambda 15 UV/vis spectrophotometer and plotted by using the Lambda computer. The slope of the linear part of increase in absorbance is directly proportional to the amount of free DNase I. The amount of free G-actin was determined by a standard plot (0–100% inhibition of DNase I). Talin and polymerization buffer alone did not inhibit DNase I.

### 2.6. Viscometric assays

Viscometric assays were performed as described [16].

## 3. RESULTS

### 3.1. Talin purification

As judged by SDS gels, talin can be isolated from platelets with 95–98% purity. On a final Sepharose CL6B gel filtration column, talin elutes in two peaks: (i) a less protein rich monomeric fraction eluting around an apparent *M*-range of 240 kDa and (ii) a higher molecular weight fraction eluting in the void volume which contains talin oligomers or aggregates (Fig. 1). An F-actin viscosity reducing activity is found to be maximal in the monomeric fraction whereas this activity appears to be reduced in the high molecular mass fraction of talin aggregates (Fig. 1). The residual viscosity reducing activity in this peak may be attributed to dissociating talin monomers at equilibrium, since on an additional gel filtration column this fraction again divides into a monomeric and a higher molecular mass pool (not shown). Experiments have been carried out exclusively with the highly purified, monomeric talin fraction.

### 3.2. Fluorescence measurements

Actin (total concentration 1.4  $\mu\text{M}$ ) containing 5% labelled NBD-actin was used to follow polymerization kinetics in the presence and absence of talin. In control samples of pure actin, filament formation and elongation is expressed as fluorescence increase over time (Fig. 2B). Nucleation, indicated by a stable fluorescence emission for approx. 50 s is followed by filament formation indicated by fluorescence increase and reaches steady-state at about 15 min. The sigmoidal curve with an initial lag phase reflects all signs of cooperativity during actin assembly under polymerization conditions. This effect disappears in the presence of talin, as was noticed also for other nucleating proteins [17]. In the

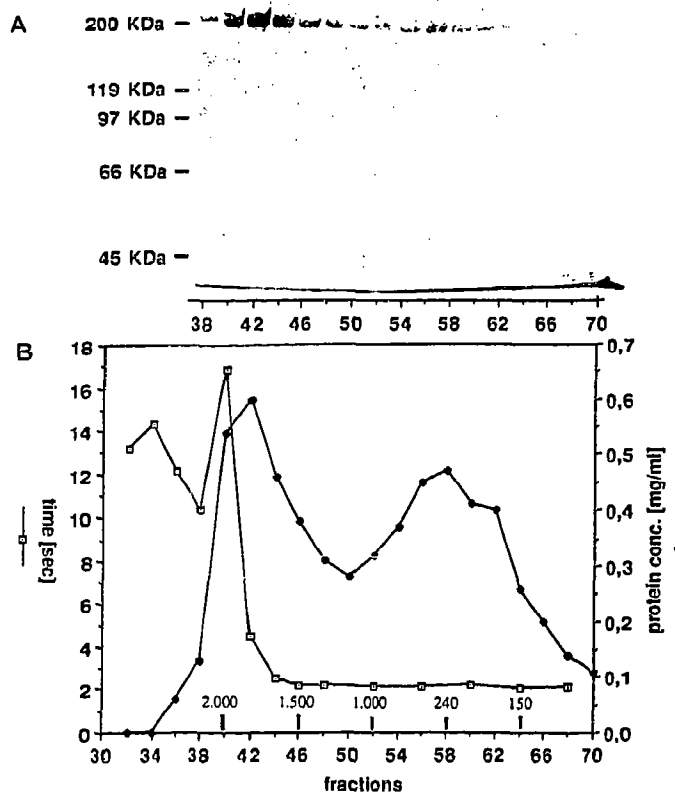


Fig. 1. Purification of platelet talin. The isolation protocol includes a final gel-filtration column from which talin elutes in two fractions: (i) a monomeric and (ii) an oligomeric form (void volume) Viscosity-reducing activity mainly resides in the monomeric fraction (B). Corresponding SDS gels are shown in (A).

presence of talin at a 1:1 molar ratio to actin, polymerization starts immediately without an apparent lag phase with a 2-fold increase in fluorescence before reaching a steady-state in approx. 10 min (Fig. 2A). The increase of steady-state fluorescence in the presence of talin results from an increase in filament number rather than in filament length as follows from the data obtained by FRAP and dynamic light scattering (see below).

### 3.3. Fluorescence titration

The dependence of the rate of actin polymerization on the talin concentration led to the calculation of the binding constant ( $K_d$ ) of talin to actin by steady-state titration. In these experiments 0.2  $\mu\text{M}$  of 100% labelled NBD-actin in G-buffer was mixed with talin at increasing concentrations up to 3  $\mu\text{M}$ . The overall equilibrium binding constant of 0.3  $\mu\text{M}$  deduced from the titration curve fitted a single exponential. However, the break-point titration (data not shown) revealed a stoichiometry of 3:1, which would indicate the existence of three individual binding sites for actin. The measurement of each individual binding constant would therefore require a transient kinetic analysis.

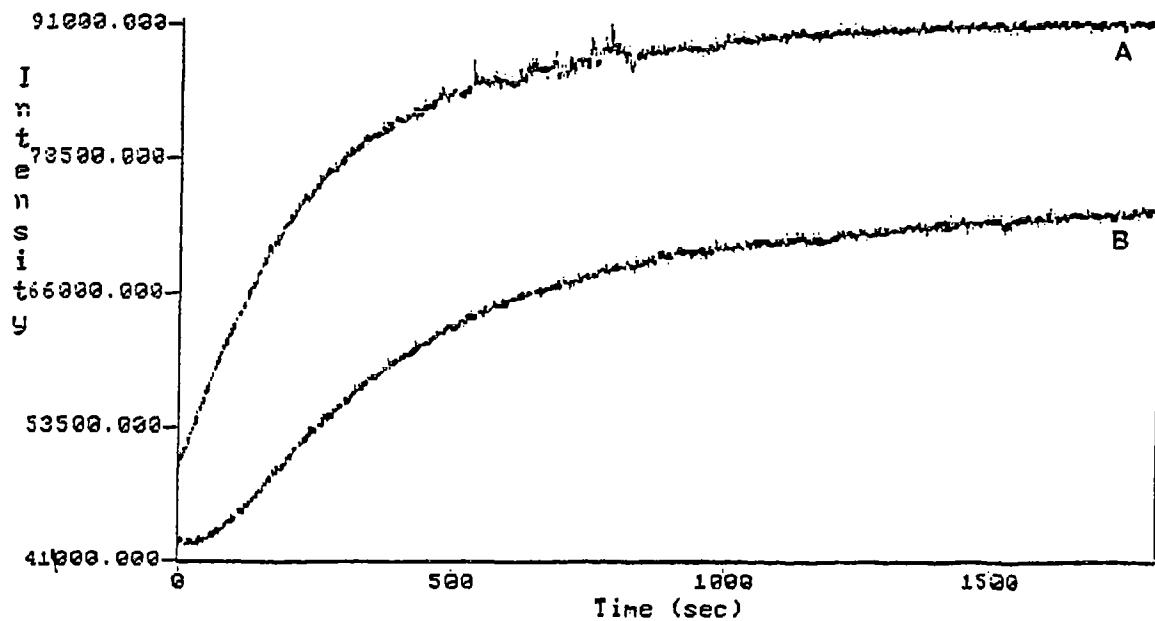


Fig. 2. Fluorescent traces of polymerizing NBD-labelled actin ( $1.4 \mu\text{M}$ ) in the absence (B) and presence (A) of talin in a 1:1 molar ratio. Note the profound reduction of nucleation time, the increase of the net polymerization rate and the increase of steady-state fluorescence.

### 3.4. Fluorescence recovery after photobleaching (FRAP)

FRAP experiments were performed in F-actin solutions to which talin was added with increasing molar ratios prior to polymerization. In Fig. 3A the relaxation time  $\tau_d$  is plotted against the molar ratio of talin to actin. For comparison, the effect of *Dictyostelium* severin is monitored under identical conditions, except that 2 mM  $\text{CaCl}_2$  (final concentration) was added to activate severin. The concentration-dependent decrease of relaxation times parallels an increase of diffusion coefficients which are greatly enhanced with the progressive formation of short actin filaments.

### 3.5. Dynamic light scattering

Dynamic light scattering was performed on F-actin (0.1 mg/ml) solutions incubated with talin at various molar ratios prior to polymerization. The initial decay of photon correlation functions recorded at a scattering angle  $\vartheta = 90^\circ$  are plotted in Fig. 3B. With actin alone, the correlation function entirely reflects internal motions of the filaments and can well be described by the Rouse-Zimm model [14]. In a population of shortened filaments center of mass diffusion leads to a steeper initial drop. With very short filaments (dilute solution), the internal modes can be neglected, and the correlation function can be described as a sum of exponential terms, each corresponding to a certain chain length

$$g(t) = \sum_l a_l \exp(-q^2 D_l t)$$

where  $a_l$  is the relative scattering intensity,  $D_l$  the diffusion coefficient of chains of length  $L$ . The steeper

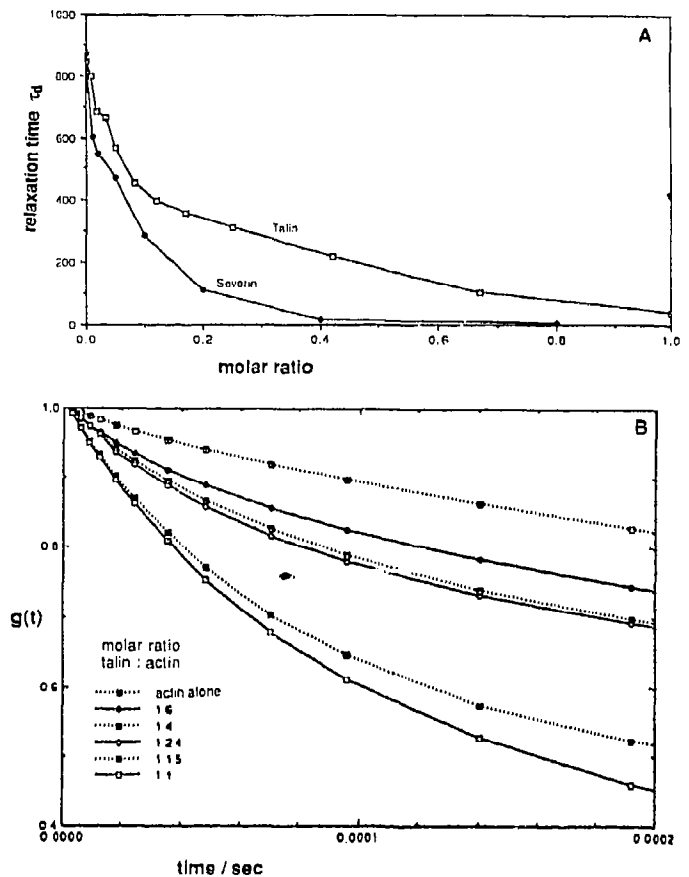


Fig. 3. Effect of talin on actin polymerization as monitored by FRAP (A) and dynamic light scattering (B). A. Relaxation times of fluorescence recovery of NBD labelled F-actin at increasing molar ratios of talin and severin, respectively. B. The photon correlation functions reflect a progressive shortening of actin filaments with increasing talin concentrations.

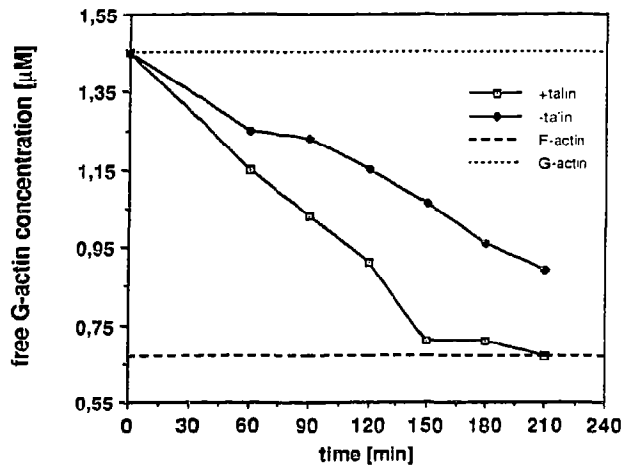


Fig. 4. Determination of the free G-actin concentration by the DNase I inhibition assay. Actin is polymerized in the presence (□ - □ - □) and absence (● - ● - ●) of talin (1:1 molar ratio). Note the rapid consumption of actin monomers, when polymerization is started in the presence of talin.

decay of photon correlation functions with increasing molar fractions of talin added prior to polymerization indicates that the number concentration of short actin filaments must have increased with raising talin concentrations.

### 3.6. DNase-I binding assay

We have measured the free G-actin concentration during actin polymerization in the presence and absence of talin by the DNase I inhibition assay (Fig. 4). Polymerization was started at a  $1.45 \mu\text{M}$  free G-actin concentration (full inhibition of DNase I). With progressing polymerization and a corresponding consumption of actin monomers, the DNase inhibition is reduced until the system reaches steady state (approx. after 6 h at this concentration). In the presence of talin (molar ratio 1:1) a pronounced decrease of the free G-actin concentration is detectable, which plateaus after 150 min at  $0.65 \mu\text{M}$ , the free G-actin concentration reached when polymerization is complete ( $\approx$  a 50% reduction of DNase inhibition). The data support a nucleating activity of talin.

Filament capping which would be reflected by an increase of the free G-actin concentration at steady state, was not observed. Under G-buffer conditions the incubation with talin up to 3 h (data not shown) did not lead to any detectable reduction of DNase inhibition, which however does not argue against a talin-G-actin complex formation. Talin alone, F-buffer or G-buffer did not cause any measurable effect on DNase I.

## 4. DISCUSSION

Surprisingly enough, talin was not recognized to bind to actin. Here, we show by four detection methods that

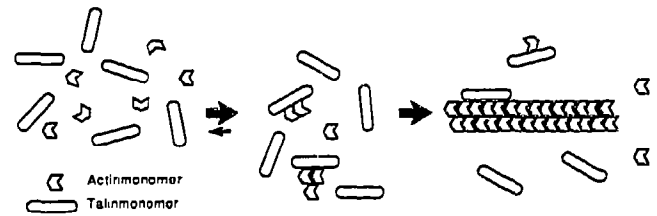


Fig. 5. Schematic view of talin-actin interaction in vitro. With a maximal binding capacity of 1:3 (molar ratio) talin promotes filament nucleation, the rate-limiting step during actin polymerization. Once nuclei have formed, polymerization is rapidly progressing.

talin is an actin binding protein in vitro, and influences actin polymerization by its nucleating activity (Fig. 5). Initially, platelet talin was recognized as P-235 a protein which according to Collier and Wang [7] restricts the length of actin filaments. Though the basic observations (suppressed relative viscosity under low shear conditions; netto reduction of filament length at steady state) were correct, the mechanism of talin action has to be interpreted adequately in the light of the present data in as much as due to the assay conditions a nucleating activity of talin has been overlooked before. When talin is added to actin in vitro, a net shortening of actin filaments is not induced by severing or capping but rather results from the increase of nucleation sites and the formation of many short filaments. This agrees well with the previous notion, that talin has only an effect on actin polymerization when added prior to polymerization but has no effect when added to preformed filaments [7].

The finding that talin can bind to actin and on the other hand selectively interacts with lipids of the plasma membrane [6] makes it an interesting protein to study the linkage of the actin cytoskeleton to biological interfaces [1]. Experiments are in progress to evaluate the kinetics of talin-actin interactions in more detail.

*Acknowledgements:* This study was supported by the Deutsche Forschungsgemeinschaft Grant Is 25/5-2. We thank Mrs. Kirpal for technical assistance and Dr E. Sackmann for discussions and the use of his technical equipment.

## REFERENCES

- [1] Isenberg, G. (1991) *J. Muscle Res. Cell Motil.* 11, in press.
- [2] Beckerle, M.C. and Yeh, R.K. (1990) *Cell Motil. Cytoskeleton* 16, 7-13.
- [3] Beckerle, M.C., Miller, D.E., Bertagnolli, M.E. and Locke, S.J. (1989) *J. Cell Biol.* 109, 3333-3346.
- [4] Isenberg, M.W. (1988) *J. Cell Biol.* 107, 256a.
- [5] O'Halloran, O., Beckerle, M.C. and Burridge, K. (1985) *Nature* 317, 449-451.
- [6] Heise, H., Bayerl, T., Isenberg, G. and Sackmann, E. (1991) *Biochim. Biophys. Acta* 1061, 121-131.
- [7] Collier, N.C. and Wang, K. (1982) *FEBS Lett.* 143, 205-210.
- [8] Spudis, J.A. and Watt, S. (1971) *J. Biol. Chem.* 246, 4866-4871.

- [9] MacLean-Fletcher, S. and Pollard, T.D. (1980) *Biochem. Biophys. Res. Commun.* 96, 18-27.
- [10] Bradford, M. (1976) *Anal. Biochem.* 72, 248-254.
- [11] Laemmli, U.K. (1970) *Nature* 227, 680-685.
- [12] Detmers, P., Weber, A., Elzinga, M. and Stephens, R.E. (1981) *J. Biol. Chem.* 256, 99-104.
- [13] Gaub, H.E., Sackmann, E., Büschl, R. and Ringsdorf, H. (1984) *Biophys. J.* 45, 725-731.
- [14] Schmidt, C.F., Bärmann, M., Isenberg, G. and Sackmann, E. (1989) *Macromolecules* 22, 3638-3649.
- [15] Blickstadt, I., Markey, F., Carlsson, L., Persson, T. and Lindberg, U. (1978) *Cell* 15, 935-943.
- [16] MacLean-Fletcher, S. and Pollard, T.D. (1980) *J. Cell Biol.* 85, 414.
- [17] Gaertner, A., Ruhnau, K., Schöer, E., Selve, N., Wanger, M. and Wegner, A. (1989) *J. Muscle Res. Cell Motil.* 10, 1-9.

*Note added in proof*

When our studies were completed we learnt that Muguruma et al. (1990) *Biochem. Biophys. Res. Commun.* 171, 1217-1223, reached similar conclusions by applying different methods.